

Relationship between Covalence and Displacive Phase Transition Temperature in RAO_4 and $LiAO_3$ ($R =$ Rare-Earth Element and $A = Nb$ and Ta)

S. Tsunekawa,* T. Kamiyama,† H. Asano,† and T. Fukuda*

*Institute for Materials Research, Tohoku University, Sendai 980-77, Japan; and †Institute of Materials Science, University of Tsukuba, Tsukuba 305, Japan

Received December 14, 1993; in revised form July 19, 1994; accepted July 21, 1994

Crystal structure analyses by TOF neutron powder diffraction are performed for $RTaO_4$ ($R =$ rare-earth element) and the Ta–O interatomic distances are determined. The relationship between the covalency of A–O bonds ($A = Nb$ and Ta), which show the most shortening upon phase transition, and the transition temperature is discussed for RAO_4 and $LiAO_3$, and the parameters of Ta–O covalence are determined. © 1995 Academic Press, Inc.

(see Fig. 1a), the Nb^{5+} ions have a larger displacement (0.3986 Å) than do the Ta^{5+} ions (0.334 Å) (6) and the AKJ relationship is not satisfied.¹ The AKJ relationship is obeyed only when η is measured from the center of the tetrahedron; if it is measured from the center of the octahedron, T_c and η^2 are anticorrelated. Specifically, for isostructural compounds of species 1 and 2 we get from Eq. [1]

INTRODUCTION

The low-temperature monoclinic phases of rare-earth orthoniobates ($RNbO_4$, $R = Y$ and La to Lu) and of rare-earth orthotantalates ($RTaO_4$, $R = Nd$ to Er) have been reported to have the space group $I2/c (= C2/c)$ (1–3) and are usually called the M phase of fergusonite. All of them have a high-temperature phase with the scheelite structure (space group $I4_1/a$). The structural transition of these materials from scheelite to fergusonite is antidisplacive and ferroelastic rather than ferroelectric. The origin of the displacive phase transition is known to be soft mode. Recently a softening of elastic moduli has been found for the ferroelastic phase transition of $LaNbO_4$ (4). However, the atomic displacement of the center cations always arises in the transition. It has been considered that the fergusonite structure needs NbO_4 or TaO_4 tetrahedra to satisfy the Abrahams–Kurtz–Jamieson (AKJ) relationship (5) between phase transition temperature, T_c , and saturated atomic displacement, η , (6); the relationship is expressed by the equation

$$T_c = C\eta^2, \quad [1]$$

where C is a constant for the isostructural system of materials. When the fergusonite structure in $NdAO_4$ ($CA = Nb$ and Ta) is viewed in terms of edge-shared octahedra

$$(T_c)_1/(T_c)_2 = (\eta^2)_1/(\eta^2)_2. \quad [2]$$

We have the following invalid results for the edge-shared octahedral structure (the M' phase of fergusonite) of $NdNbO_4$ and $NdTaO_4$:

$$(T_c)_{Nb}/(T_c)_{Ta} = 998 \text{ K}/1601 \text{ K} = 0.623 \quad [3]$$

and

$$(\eta^2)_{Nb}/(\eta^2)_{Ta} = (0.3986 \text{ Å})^2/(0.334 \text{ Å})^2 = 1.424. \quad [4]$$

On the other hand, it is found that the Nb^{5+} ion has the smaller displacement, 0.2346 Å, in comparison with 0.298 Å for the Ta^{5+} ion (6)², if displacement from the centers of the oxygen tetrahedra is considered, and we get

$$(\eta^2)_{Nb}/(\eta^2)_{Ta} = (0.2346 \text{ Å})^2/(0.298 \text{ Å})^2 = 0.620. \quad [5]$$

¹ Although the displacements calculated from our crystal structure data (see (8) and Table I in this paper) are 0.3174 Å for Nb^{5+} ions and 0.3287 Å for Ta^{5+} , the AKJ relationship is not satisfied.

² Our results obtained from the above crystal structure data are 0.1755 Å for Nb^{5+} ions and 0.2223 Å for Ta^{5+} ions.

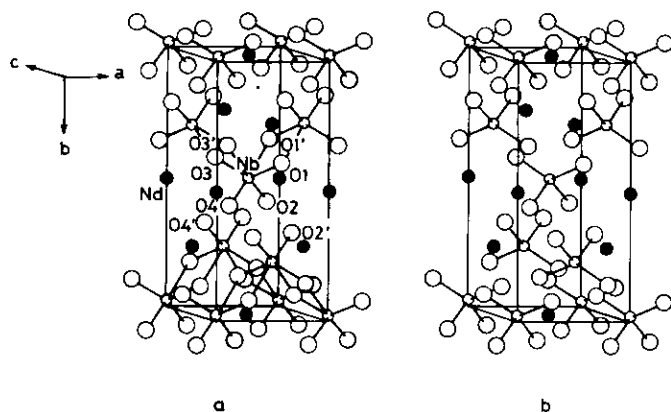


FIG. 1. The monoclinic fergusonite structure of NdNbO_4 described in terms of (a) edge-shared octahedra (called the M' phase) and (b) isolated tetrahedra (called the M phase) (6): Nd (●), Nb (○), and O (○).

Therefore, Eq. [2] holds only in the case of the isolated tetrahedral structure (the M phase of fergusonite).

However, David (7) illustrated for LaNbO_4 crystals that the oxygen atoms of the fifth and sixth shortest bonds around niobium ions in the low-temperature monoclinic phase, which are the second nearest neighbor atoms in the high-temperature tetragonal phase, are responsible for the ferroelastic phase transition; the driving force for Nb^{5+} ions to transfer to off-center positions during the transition arises from the remarkable approach of oxygen atoms $\text{O1}'$ and $\text{O3}'$ to become the fifth and sixth shortest bonds (see Fig. 1b).

Recently we have performed structural analyses of RNbO_4 ($R = \text{La, Nd, Ho, and Yb}$) (8) and RTaO_4 ($R = \text{Nd and Ho}$) by neutron powder diffraction. In this paper, we elucidate the above problem in terms of bond valence. We discuss the relationship between the covalence of particular $A\text{-O}$ bonds ($A = \text{Nb and Ta}$) and the phase transition temperature and determine the parameters of Ta-O covalence.

EXPERIMENTAL AND RESULTS

Powder samples of RTaO_4 crystals ($R = \text{Nd and Ho}$) grown by the floating zone method were prepared by the same method as previously reported for RNbO_4 ($R = \text{La, Nd, Ho, and Yb}$) (8). Neutron powder diffraction experiments were carried out at room temperature with a TOF (time-of-flight) neutron powder diffractometer at the KENS pulsed neutron source in the National Laboratory for High Energy Physics at Tsukuba. Intensity data were collected using 12 ^3He counters installed at an average 2θ of 170° . The resolution of the diffractometer, $\Delta d/d$, was 3×10^{-3} . These data were refined by the Rietveld method using the program RIETAN (9). The number of parameters refined was 50 (47 for HoTaO_4). The profile

function is described by the modified Cole-Windsor function (10) with 10 parameters; it has a Gaussian leading edge, another Gaussian peak, and an exponentially decaying tail. The tail has two components with different decay constants, whose ratio is a function of neutron wavelength (9). The background is described by a polynomial with six background parameters multiplied by the incident neutron spectrum (9). Refinements included roughly 1200 reflections over the range of d spacings from 0.5 to 3.3 Å. The values of coherent scattering lengths used for the refinements were 7.80 (Nd), 8.50 (Ho) (11), 6.91 (Ta), and 5.803 (O) (12) in units of fm ($=10^{-13}$ cm).

Rietveld refinement patterns of RTaO_4 ($R = \text{Nd and Ho}$) based on space group symmetry $I2/c$ have good fits, as shown in Fig. 2. Final R factors and structure parameters are listed in Table 1. In the case of Ta in HoTaO_4 , U_{11} had a slightly negative value in the anisotropic refinement, and therefore we refined the isotropic thermal parameter. The values of Ta-O interatomic distances and O-Ta-O angles calculated with the program ORFFE (13) are given in Table 2 along with Nb-O distances and O-Nb-O angles.

DISCUSSION

A neutron powder diffraction analysis of NdTaO_4 at room temperature has been reported by Santro *et al.* (14). However, their result is less accurate than ours: they obtained a goodness-of-fit indicator (15) of $R_{\text{wp}}/R_e = 1.52$, in comparison with our indicator of 1.06, where the values used are $R_{\text{wp}} = 10.70\%$ and $R_e = 7.06\%$ for Santro *et al.* (14) and $R_{\text{wp}} = 2.97\%$ and $R_e = 2.79\%$ for our work (Table 1). Reliable atomic positions are required for discussing bond valence.

David (6) has indicated that the AKJ relationship shown in ferroelectric LiAO_3 is similarly applied to ferroelastic NdAO_4 in terms of isolated AO_4 tetrahedra ($A = \text{Nb and Ta}$). The AKJ relationship connects the saturated displacement of center cations with the phase transition temperature, T_c , from the viewpoint of energetics. We discuss the relationship between the bonding nature and T_c using two approaches to the chemical bonding. One is to investigate the correlation between the bond valence sum (BVS) and T_c , and the other is to investigate the correlation between the bond valence (BV) of a particular bond and T_c .

We show in Table 3 the values of the bond valence, s_j , of the eight $A\text{-O}$ bonds for RAO_4 ($R = \text{Nd and Ho}$) obtained by the bond valence equation of Brown and Altermatt (16) and of the bond valence sum, S , together with their phase transition temperature. BV of the j th bond is defined by

$$s_j = \exp[(R_0 - R_j)/0.37], \quad [6]$$

and BVS is defined by

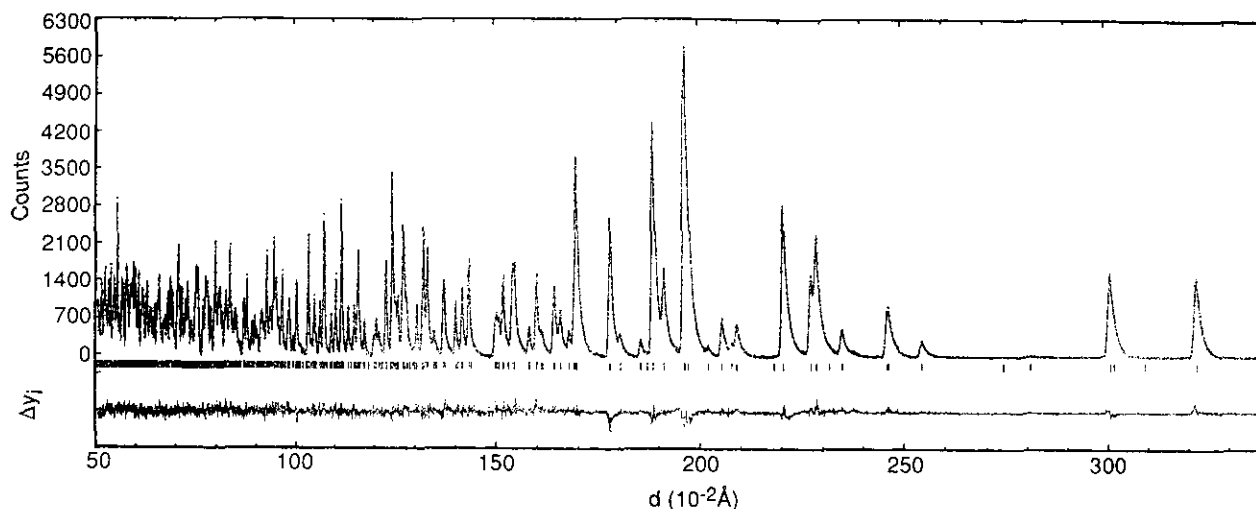


FIG. 2. Rietveld refinement pattern of the HRP data for NdTaO_4 . Observed intensity data are shown by dots and the solid line overlying them is the calculated intensity. Vertical markers below the diffraction pattern indicate the positions of 1293 possible reflections. ΔI_i in the bottom is the difference between observed and calculated intensities. The background is subtracted before plotting.

$$S = \sum s_j, \quad [7]$$

where R_j is the interatomic distance, and $R_0 = 1.911$ and 1.920 \AA , respectively, for Nb–O and Ta–O bonds. In the table, BV and BVS for LiNbO_3 and LiTaO_3 are listed also; these have NbO_6 octahedra (17) and TaO_6 octahedra (18).

Most recently the correlation between ionicity and BVS has been reported by Tanaka (19); ionicity ($=1 - \text{covalency}$) decreases with the increase in the BVS. We look

for a correlation between BVS and T_c using the values in Table 3. We can note qualitative proportionality between BVS and T_c for both RNbO_4 and RTaO_4 , but no such tendency exists for LiNbO_3 and LiTaO_3 .

Brown and Shannon (20) have discussed the relationship between BV and covalence, f'_c . For the covalence of the j th bond,

$$(f'_c)_j = a s_j^M, \quad [8]$$

TABLE 1
Structure Parameters for RTaO_4 ($R = \text{Nd}$ and Ho) at Room Temperature^a

Atom	Site	x	y	z	U_{11}	U_{22}	U_{33}	U_{12}	U_{13}	U_{23}	B_{eq}
NdTaO_4 ($I2/c$) $R_{\text{wp}} = 2.97\%$, $R_p = 2.30\%$, $R_c = 2.79\%$, $R_I = 2.49\%$, $R_F = 1.25\%$ ^b $a = 5.5164(1) \text{ \AA}$, $b = 11.2412(2) \text{ \AA}$, $c = 5.1176(1) \text{ \AA}$, $\beta = 95.717(1)^\circ$											
Nd	4e	0	0.6322(1)	$\frac{1}{4}$	0.0013(4)	0.0020(4)	0.0034(4)	0	0.0003(3)	0	0.18
Ta	4e	0	0.0988(1)	$\frac{1}{4}$	0.0028(5)	0.0034(5)	0.0027(5)	0	0.0008(4)	0	0.24
O(1)	8f	0.2353(2)	0.0314(1)	0.0331(2)	0.0062(4)	0.0047(4)	0.0071(4)	0.0015(4)	0.0049(3)	0.0011(3)	0.47
O(2)	8f	0.1498(2)	0.2056(1)	0.4893(2)	0.0047(4)	0.0064(4)	0.0062(4)	-0.0003(4)	-0.0012(3)	-0.0026(3)	0.46
HoTaO_4 ($I2/c$) $R_{\text{wp}} = 2.85\%$, $R_p = 2.26\%$, $R_c = 2.61\%$, $R_I = 3.24\%$, $R_F = 1.34\%$ $a = 5.3291(1) \text{ \AA}$, $b = 10.9329(2) \text{ \AA}$, $c = 5.0548(1) \text{ \AA}$, $\beta = 95.524(1)^\circ$											
Ho	4e	0	0.6320(1)	$\frac{1}{4}$	0.0027(4)	0.0030(5)	0.0018(4)	0	0.0005(3)	0	0.20
Ta	4e	0	0.1018(1)	$\frac{1}{4}$	—	—	—	—	—	—	0.11(2)
O(1)	8f	0.2424(2)	0.0309(1)	0.0294(2)	0.0040(4)	0.0032(5)	0.0048(5)	0.0001(4)	0.0017(4)	-0.0002(4)	0.32
O(2)	8f	0.1556(2)	0.2094(1)	0.4960(2)	0.0039(4)	0.0053(5)	0.0056(5)	-0.0006(4)	-0.0001(3)	-0.0021(4)	0.39

^a Refer to the previous paper (8) for RNbO_4 ($R = \text{La}$, Nd , Ho , and Yb). $U_{ij} (\text{\AA}^2)$ is the anisotropic thermal parameter, and $B_{\text{eq}} (\text{\AA}^2)$ is the equivalent isotropic thermal parameter. Numbers in parentheses are estimated standard deviations of the last significant digit.

^b R_{wp} and R_p are defined for all the data points in the profile with and without a weighting factor, respectively. R_I and R_F are respectively for the integrated Bragg intensity and the structure factor. R_c is an expected R factor.

TABLE 2
Interatomic Distances A–O and O–A–O Angles (A = Nb and Ta) in RAO_4 (R = Nd and Ho)^a

Sample		Interatomic distance (Å)				Angle (°)			
		A–O1 (=A–O3)	A–O2 (=A–O4)	A–O1' (=A–O3')	A–O2' (=A–O4')	O1–A–O3	O2–A–O4	O1'–A–O3'	O2'–A–O4' ^b
NdAO ₄	A = Nb	1.918(1) × 2	1.842(1) × 2	2.473(1) × 2	3.180(1) × 2	130.36(7)	102.22(7)	109.96(7)	100.71(4)
	A = Ta	1.944(1) × 2	1.851(1) × 2	2.356(1) × 2	3.246(1) × 2	134.14(8)	99.02(8)	110.57(5)	98.89(5)
HoAO ₄	A = Nb	1.919(1) × 2	1.841(1) × 2	2.424(1) × 2	3.049(1) × 2	130.31(8)	103.65(8)	110.23(4)	99.99(4)
	A = Ta	1.947(1) × 2	1.849(1) × 2	2.327(2) × 2	3.101(2) × 2	133.0(1)	101.0(1)	111.05(5)	98.49(6)

^a Refer to Fig. 1 for labeling of the oxygen atoms.

^b For simplicity, A–O(1), A–O(2), etc., are expressed as A–O1, A–O2, etc.

where the covalence parameters a and M have the same values for cations with 18, 36, and 54 electrons in their core: $a = 0.49$ v.u. and $M = 1.57$ (Nb⁵⁺ ions have 36 electrons in their core), where v.u. denotes valence unit. However, the parameters of Ta⁵⁺ ions, which have 68 electrons, were not mentioned.

We consider that the covalence of the fifth and sixth shortest bonds, A–O1' and A–O3' (A–O1' = A–O3' and A = Nb and Ta), correlates with T_c , because two Nb–O

bond lengths in LaNbO₄, 1.862 Å (× 4) and 2.971 Å (× 4), in the high-temperature tetragonal phase at 803 K (7) split into four lengths, 1.824 Å (× 2), 1.917 Å (× 2), 2.540 Å (× 2), and 3.259 Å (× 2), in the low-temperature monoclinic phase at room temperature (21) and the A–O1' bonds show the most shortening. The values of covalence, (f'_j), and covalency, C_j , for the j th bond length most shortened are shown in Table 4. The covalency is defined by the equation

$$C_j = (f'_j)/s_j (= as_j^{M-1}), \quad [9]$$

TABLE 3
Bond Valence, s_j , Bond Valence Sum, S , and Phase Transition Temperature, T_c , of $RNbO_4$ and $RTaO_4$ (R = Nd and Ho)^a

Sample	j	R_j (Å)	s_j (v.u.)	S (v.u.)	T_c (K)
NdNbO ₄	1	1.842(1) × 2	1.205(3)	4.875(3)	998(5) ^b
	2	1.918(1) × 2	0.981(3)		
	3	2.473(1) × 2	0.2189(6)		
	4	3.180(1) × 2	0.0324(1)		
HoNbO ₄	1	1.841(1) × 2	1.208(3)	4.966(3)	1088
	2	1.919(1) × 2	0.979(3)		
	3	2.424(1) × 2	0.2500(7)		
	4	3.049(1) × 2	0.0462(1)		
LiNbO ₃	1	1.889(3) × 3	1.061(9)	4.93(2)	1468(15) ^c
	2	2.112(4) × 3	0.581(6)		
NdTaO ₄	1	1.851(1) × 2	1.205(3)	4.955(3)	1601
	2	1.944(1) × 2	0.937(3)		
	3	2.356(1) × 2	0.3078(8)		
	4	3.246(1) × 2	0.0278(1)		
HoTaO ₄	1	1.849(1) × 2	1.212(3)	5.032(3)	1681
	2	1.947(1) × 2	0.930(3)		
	3	2.327(2) × 2	0.3329(9)		
	4	3.101(2) × 2	0.0411(2)		
LiTaO ₃	1	1.908(3) × 3	1.033(8)	5.08(1)	891(5) ^c
	2	2.073(3) × 3	0.661(5)		

^a Interatomic distances, R_j 's, of LiNbO₃ and LiTaO₃ were obtained from Refs. (17) and (18), respectively.

^b See Ref. (24).

^c See Ref. (25).

where $j = 3$ for $RNbO_4$ and $RTaO_4$, and $j = 1$ for LiNbO₃ and LiTaO₃, because six equal Nb–O bond lengths in LiNbO₃, 1.911 Å, in the high-temperature phase at 1473 K split into two different lengths, 1.889 Å (× 3) and 2.112 Å (× 3), in the low-temperature phase at room temperature (22) (see Table 3).

TABLE 4
Covalence, f'_j , and Covalency, C_j , of the j th A–O Bond in RAO_4 and $LiAO_3$ (R = Rare-Earth Element and A = Nb and Ta) Crystals, and the Phase Transition Temperature, T_c ^a

Sample	j	s_j (v.u.)	(f'_j) _{j} (v.u.)	C_j (%)	T_c (K)		
$RNbO_4$	R = La	3	0.182(1)	0.0337(3)	18.54(6)	768(5)	
		Nd	3	0.2189(6)	0.0451(2)	20.61(3)	998(5)
		Ho	3	0.2500(7)	0.0556(2)	22.23(4)	1088
		Yb	3	0.262(1)	0.0600(4)	22.86(5)	1098
LiNbO ₃	1	1.061(9)	0.538(7)	50.7(2)	1468(15)		
$RTaO_4$	R = Nd	3	0.3078(8)	[0.08917]	[29.0]	1601	
		Ho	3	0.3329(9)	[0.09988]	[30.0]	1681
		LiTaO ₃	1	1.033(8)	[0.5028]	[48.7]	891(5)

^a Numerical values estimated with the parameters of Ta–O covalence are shown in brackets.

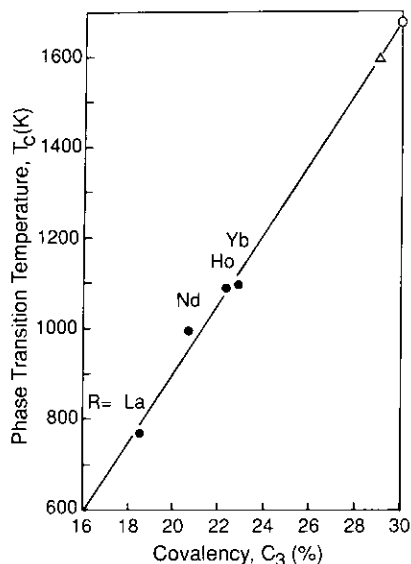


FIG. 3. Relationship between covalency and phase transition temperature of rare-earth orthoniobates ($RNbO_4$, $R = La, Nd, Ho,$ and Yb) (●) and of rare-earth orthotantalates, $NdTaO_4$ (Δ) and $HoTaO_4$ (○).

We obtain a linear relation by the least-squares method as shown in Fig. 3, plotting the covalencies of $RNbO_4$ ($R = La, Nd, Ho,$ and Yb) versus their phase transition temperatures shown in Table 4. Assuming that the same relation holds for $RTaO_4$ ($R = Nd,$ and Ho), we get the covalencies of 29.0% for $NdTaO_4$ and 30.0% for $HoTaO_4$. Substituting these values and the BV of the Ta–O1' bonds into Eq. [9], we obtain the parameters of $a = 0.48$ v.u. and $M = 1.43$ that are those for the number of electrons in the core, 68. Applying these parameters to the BV of the first nearest Ta–O bonds in $LiTaO_3$, we get the values 0.5028 for covalence and 48.7% for covalency (see Table 4). These results indicate that the increase in covalency of 1% for RAO_4 corresponds to the T_c elevation of 80 K, whereas that for $LiAO_3$ corresponds to 290 K ($A = Nb$ and Ta).

It is noted that C_j of $HoTaO_4$ is the highest among the $RNbO_4$ ($R = La, Nd, Ho,$ and Yb) and $RTaO_4$ ($R = Nd$ and Ho) in Table 4. Over 30% covalency of the A–O1' bonds may be necessary for the modification from the M to M' phase of fergusonite (see Table 4), because the M' phase appears only in sintered $HoTaO_4$ (23). More extensive studies on the crystals with the M' phase are required to clarify the correlation between the covalency and the appearance of the M' phase.

CONCLUSION

The Ta–O interatomic distances in $RTaO_4$ ($R = Nd$ and Ho) were obtained by neutron powder diffraction, and their bond valences and the bond valence sums were estimated along with those of $LiNbO_3$ and $LiTaO_3$. A linear

relation was found between covalencies of the Nb–O1' bonds in $RNbO_4$ ($R = La, Nd, Ho,$ and Yb) and their phase transition temperatures. Assuming that the same relation exists in $RTaO_4$, unknown covalence parameters for Ta–O bonds were estimated as $a = 0.48$ v.u. and $M = 1.43$. It was found that the elevation of T_c with an increase in covalency of 1% is 80 K for RAO_4 and 290 K for $LiAO_3$ ($A = Nb$ and Ta) with the use of these parameters.

ACKNOWLEDGMENT

The authors express their thanks to Mr. K. Sasaki of the Institute for Materials Research at Tohoku University for his help in growing the single crystals.

REFERENCES

1. L. H. Brixner, J. F. Whitney, F. C. Zumsteg, and G. A. Jones, *Mater. Res. Bull.* **12**, 17 (1977).
2. M. Tanaka, R. Saito, and D. Watanabe, *Acta Crystallogr. Sect. A* **36**, 350 (1980).
3. C. Keller, *Z. Anorg. Allg. Chem.* **318**, 89 (1962).
4. K. Hara, A. Sasaki, S. Tsunekawa, A. Sawada, Y. Ishibashi, and T. Yagi, *J. Phys. Soc. Jpn.* **54**, 1168 (1985).
5. S. C. Abrahams, S. K. Kurtz, and P. B. Jamieson, *Phys. Rev.* **172**, 551 (1968).
6. W. I. F. David, *Mater. Res. Bull.* **18**, 809 (1983).
7. W. I. F. David, *Mater. Res. Bull.* **18**, 749 (1983).
8. S. Tsunekawa, T. Kamiyama, K. Sasaki, H. Asano, and T. Fukuda, *Acta Crystallogr. Sect. A* **49**, 595 (1993).
9. F. Izumi, H. Asano, H. Murata, and N. Watanabe, *J. Appl. Crystallogr.* **20**, 411 (1987).
10. I. Cole and C. G. Windsor, *Nucl. Instrum. Methods.* **171**, 107 (1980).
11. C. G. Windsor, "Pulsed Neutron Scattering," p. 407. Taylor & Francis, London, 1981.
12. V. F. Sears, in "International Tables for Crystallography, Vol. C" (A. J. C. Wilson, Ed.), p. 383. Kluwer, Dordrecht, 1992.
13. W. R. Busing, K. O. Martin, and H. A. Levy, Report ORNL-TM-306. Oak Ridge National Laboratory, Oak Ridge, TN, 1964.
14. A. Santoro, M. Marezio, R. S. Roth, and D. Minor, *J. Solid State Chem.* **35**, 167 (1980).
15. R. A. Young, in "The Rietveld Method" (R. A. Young, Ed.), p. 22. Oxford Univ. Press, Oxford, 1993.
16. I. D. Brown and D. Altermatt, *Acta Crystallogr. Sect. B* **41**, 244 (1985).
17. S. C. Abrahams, J. M. Reddy, and J. L. Bernstein, *J. Phys. Chem. Solids* **27**, 997 (1966).
18. S. C. Abrahams, W. C. Hamilton, and A. Sequeira, *J. Phys. Chem. Solids* **28**, 1693 (1967).
19. S. Tanaka, *Physica C* **220**, 341 (1994).
20. I. D. Brown and R. D. Shannon, *Acta Crystallogr. Sect. A* **29**, 266 (1973).
21. W. I. F. David, S. Hull, and R. M. Ibberson, Report RAL-90-024, p. 1. Rutherford Appleton Laboratory, Oxfordshire, 1990.
22. S. C. Abrahams, H. J. Levinstein, and J. M. Reddy, *J. Phys. Chem. Solids* **27**, 1019 (1966).
23. L. H. Brixner and H.-Y. Chen, *J. Electrochem. Soc.* **130**, 2435 (1983).
24. H. Takei and S. Tsunekawa, *J. Crystal Growth* **38**, 55 (1977).
25. S. C. Abrahams and J. L. Bernstein, *J. Phys. Chem. Solids* **28**, 1685 (1967).